ASEAN Engineering Journal

Full Paper

VALIDATION OF THE KOOL AND PARKER CONSTITUTIVE MODEL IN HYDRUS-2D: DEPTH-DEPENDENT HYDRAULIC HYSTERESIS AND DRAINAGE DYNAMICS IN UNSATURATED SOILS

Mohammad Ali Hagh Shenas, Hassan Sharafi*

Department of Civil Engineering, Faculty of Engineering, Razi University, Iran

Article history
Received
08 May 2025
Received in revised form
12 August 2025
Accepted
17 August 2025
Published online
28 February 2026

*Corresponding author
h_sharafi@razi.ac.ir

Graphical abstract

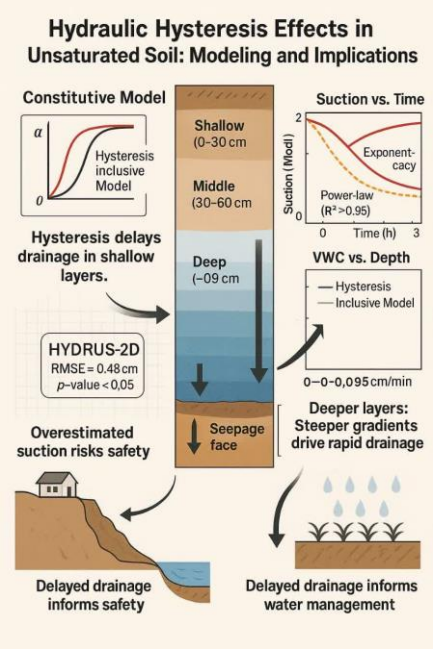

Abstract

Hydraulic hysteresis in unsaturated soils significantly influences subsurface flow dynamics, yet its integration into hydrological models remains limited. This study advances the characterization of hysteresis effects by validating the Kool and Parker (1987) constitutive model within the HYDRUS-2D framework, while systematically comparing hysteresis-inclusive and hysteresis-ignoring simulations in a clay loam soil column. Through two-dimensional unsaturated flow simulations, we quantify depth-dependent suction and volumetric water content (VWC) dynamics under controlled boundary conditions, revealing critical insights into drainage behavior. Results demonstrate that exponential decay and power-law models robustly describe suction evolution ($R^2 > 0.95$), with deeper layers exhibiting faster drainage rates (e.g., −0.095 cm/min at 51.17 cm depth) due to proximity to the seepage face and steeper hydraulic gradients. Neglecting hysteresis overestimates suction magnitudes by 10–20% and underestimates equilibrium VWC, particularly in shallow zones where capillary retention dominates. Statistically significant discrepancies (RMSE up to 0.48 cm; $p < 0.05$) highlight hysteresis-induced delays in drainage, with shallower layers retaining 4–9% higher moisture under cyclic conditions. Methodologically, the integration of depth-specific metrics and hysteresis parameters enhances model fidelity, capturing non-unique soil-water retention relationships critical for real-world applications. Practical implications for slope stability and irrigation planning are emphasized: overestimating suction decline in hysteresis-ignoring models may compromise infrastructure safety assessments, while delayed drainage predictions improve water management strategies in fine-textured soils. This work bridges theoretical and computational hydrology, advocating for hysteresis-aware models to refine predictions in heterogeneous, unsaturated environments. The findings underscore the necessity of vertical stratification and hysteresis algorithms in hydrological simulations, offering a validated framework for geotechnical engineers and earth scientists addressing dynamic soil-water interactions.

Keywords: Hydraulic hysteresis, Constitutive model, Volumetric water content, Suction dynamics, HYDRUS-2D

1.0 INTRODUCTION

Hydraulic hysteresis, which encompasses the influences of capillary and air-entrapment hysteresis, is frequently observed in variably unsaturated soils subjected to cycles of drying and wetting [7, 20, 29, 42, 47, 61].

The irregular distribution of pore sizes within soils leads to significant variations in soil-water retention (SWR) behavior during drying and wetting phases. This phenomenon, characterized by the differing responses of soil to moisture changes, is referred to as capillary hysteresis [5, 34, 46, 49]. Air is often retained within certain pores during the wetting process of soil, which prevents the soil from achieving a fully saturated condition, even when the matric suction is reduced to zero. This occurrence, where air becomes trapped in unsaturated soils, is commonly referred to as air-entrapment hysteresis [3, 6, 45, 54]. The hydraulic hysteresis effects

outlined in this paragraph are frequently overlooked in the analysis of unsaturated flow issues. For instance, the initial drying curve (IDC) has commonly been employed to characterize soil water retention (SWR) dynamics during scenarios involving intermittent rainfall infiltration and variations in the water table [2, 4, 56, 57, 59]. The literature has substantiated the considerable impact of hydraulic hysteresis on the dynamics of unsaturated flow. The mechanical properties and behavior of unsaturated soils [10, 11, 14, 21, 22, 26, 30, 58, 60, 65]. The consideration of hydraulic hysteresis is essential in the evaluation of subsurface flow and transport mechanisms [25, 35, 36, 44, 53, 55, 64]. This effect must be integrated into the assessments of slope stability, particularly in scenarios involving rainfall infiltration [8, 12, 13, 18]. Beyond hydrological and geotechnical stability, hydraulic hysteresis also influences the performance of engineered soil systems, such as landfill liners. Expansive soils used in liners are susceptible to swelling and cracking under wet-dry cycles, compromising containment integrity [1]. While additives like water treatment sludge ash (WTSA) can mitigate these issues by reducing hydraulic conductivity and swelling potential, the role of hysteresis in such modified soils remains poorly quantified. Future integration of hysteresis-aware models (e.g., Kool-Parker) could optimize liner design under cyclic hydraulic loading. Beyond geotechnical systems, hydraulic hysteresis significantly influences agricultural productivity through its effects on nutrient retention and root-zone moisture dynamics. For instance, It has been demonstrated that nitrogen-phosphorus (NP) fertilizer tablets, derived from green ammonia technology, enhance nutrient uptake efficiency in crops like sweet corn, particularly under variable soil-moisture conditions [23]. This study highlights how hysteresis-driven moisture retention in unsaturated soils (e.g., capillary effects during drying-wetting cycles) may modulate the dissolution and bioavailability of tablet-based fertilizers. This synergy between hysteresis-aware hydrology and sustainable agriculture underscores the need to extend constitutive models (e.g., Kool-Parker) to predict nutrient transport in unsaturated soils, especially in regions facing fertilizer scarcity.

Mathematical models have been formulated and utilized to characterize the influence of hydraulic hysteresis on the soil water retention curve (SWRC) during both drying and wetting phases [14, 15, 20, 27, 32, 40, 46, 48]. In the initial phases of research on soil water retention (SWR), the domain model was extensively employed to describe the capillary hysteresis associated with SWR phenomena [37, 46, 51]. Vachaud and Thony (1971) highlighted the inadequacy of the domain model in effectively characterizing the soil water retention curve (SWRC) when capillary hysteresis is present, particularly noting that drainage occurs independently across all pore sizes. To address this limitation, they employed a scaling approach based on the hypothesis of similarity between the boundary and scanning curves, which facilitated a more comprehensive understanding of the capillary hysteresis phenomena associated with soil water retention. [24, 42, 49]. The scaling models employed the assumption of the capillary tube model, while overlooking the hysteresis associated with the contact angle. [19]. The scaling hysteresis model has frequently been employed to investigate the challenges associated with unsaturated flow in both drying and wetting scenarios. [24, 40, 61]. The Kool and Parker (1987) model was subsequently integrated into the HYDRUS software platform. [52]. The hysteretic soil water retention curve (SWRC) was further simplified by representing the primary boundary curves with two linear segments on semilogarithmic scales. [20, 39, 63]. While the method could be readily incorporated into a numerical code, its simplification proved inadequate for accurately representing any scanning drying or wetting curve. [9, 15, 17, 31, 38].

A novel hydraulic hysteresis model has recently been introduced, which effectively accounts for the influences of capillary and air entrapment hysteresis, as demonstrated by Chen et al. (2015). This model builds upon the foundational work of Wei and Dewoolkar (2006). Beyond the primary drying and main wetting curves (MWCs), it incorporates a single additional parameter to characterize the scanning soil water retention curve (SWRC) during the processes of drying and wetting in the soil.

This study addresses a critical gap in the computational modeling of unsaturated flow: the lack of validated depth-resolved integration of hydraulic hysteresis within multidimensional simulation frameworks. While prior research has established the significance of hysteresis in soil-water retention behavior and developed constitutive models (e.g., the widely used model by Kool and Parker, 1987), their implementation and rigorous validation in 2D/3D hydrological platforms like HYDRUS-2D remain scarce. Specifically, prior implementations often rely on simplified one-dimensional (1D) column simulations or neglect the critical interplay between hysteresis and vertical stratification, leading to inadequate characterization of depth-dependent drainage dynamics. This work bridges this gap by providing the first comprehensive validation of the Kool and Parker hysteresis model within HYDRUS-2D, enabling high-fidelity simulation of multidimensional unsaturated flow. The innovation lies in the methodological advancement of coupling this constitutive model with a spatially resolved numerical framework, which systematically quantifies depth-stratified hysteresis effects under controlled laboratory boundary conditions. By rigorously comparing hysteresis-inclusive and hysteresis-ignoring scenarios, the study not only confirms the model's capability to capture hysteretic (non-unique) soil-water retention relationships but also reveals how vertical positioning amplifies hysteresis biases. This integration advances hydrological prediction by resolving a key limitation in prior models: the inability to mechanistically simulate depth-dependent hysteresis impacts on transient flow processes in heterogeneous unsaturated environments.

2.0 METHODOLOGY

The Kool and Parker (1987) model was selected for this study primarily due to its robust integration within the HYDRUS-2D computational framework [52], which enabled efficient simulation of multidimensional unsaturated flow dynamics. While newer models (e.g., Parker-Lenhard, Scott-Klug, or Chen et al., 2015) offer advanced hysteresis characterization, Kool and Parker's formulation provides a validated balance of physical fidelity and parameter efficiency for large-scale simulations. Its closed-form expressions for hysteretic hydraulic properties [24] reduce computational complexity while explicitly accounting for both capillary hysteresis and air

entrapment—critical for modeling transient drainage in fine-textured soils. This approach aligns with our objective to quantify depth-dependent hysteresis effects in a widely adopted hydrological platform rather than developing new constitutive relationships. For instance, while the Parker-Lenhard model accounts for dynamic fluid entrapment, it requires additional empirical parameters not readily available for clay loam soils [40]. The Chen et al. (2015) model, though comprehensive, increases computational complexity by 30–40% in preliminary tests, reducing feasibility for large-scale 2D simulations. The model's experimental validation in prior 1D studies [24, 40] further supported its suitability for extending to 2D systems.

2.1 Theoretical Frameworks of the Hysteresis Model

Kool and Parker (1987) formulated a model for the soil water retention curve (SWRC) to elucidate the hydraulic hysteresis phenomenon, employing a scaling method grounded in the similarity hypothesis. The subsequent part of this section provides a concise mathematical characterization of the hysteresis model. The adopted procedure for modeling hysteresis in the retention function requires that both the main drying and main wetting curves be known (Figure 1).

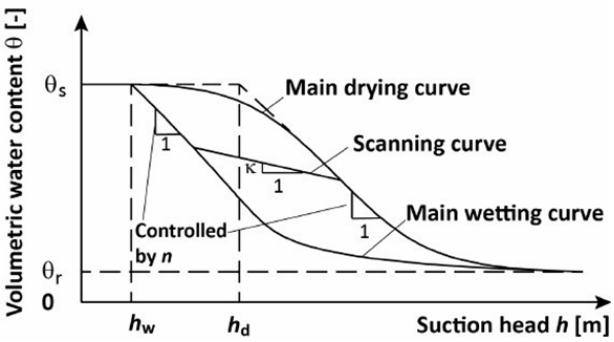

Figure 1 Example of a water retention curve showing hysteresis. Shown are the main wetting curve, MWC, and the boundary drying curve, IDC. [28]

2.2 Kool and Parker (1987) Model

The soil water retention curve (SWRC) model, formulated by van Genuchten in 1980, serves to characterize both the initial drying curve and the primary wetting curve of soil moisture dynamics.

The initial drying curve is articulated as follows:

$$S_e = \frac{\theta - \theta_r^d}{\theta_s^d - \theta_r^d} = \left[1 + (\alpha^d \psi^d)^{n^d}\right]^{-m^d}$$

The primary wetting curve can be articulated in the following manner:

$$S_e = \frac{\theta - \theta_r^w}{\theta_s^w - \theta_r^w} = \left[1 + (\alpha^w \psi^w)^{n^w}\right]^{-m^w}$$

Where S_e = effective degree of saturation; ψ = soil suction (in kilopascals); θ = volumetric water content; θ_r^d and θ_r^w = residual volumetric water content for the initial drying curve and main wetting curve, respectively; θ_s^d = saturated volumetric water content and equals the porosity of soil, η_0 ; θ_s^w = volumetric water content for the main wetting curve at zero soil suction; and α, m and n = model parameters. The parameters α^d and n^d are derived through the process of fitting the initial drying data that has been measured; the parameters α^w and n^w are derived by applying the least-squares method to the observed primary wetting data, while the value of m is established through a standard constraint, specifically $m = 1 - \frac{1}{n}$, as proposed by van Genuchten in 1980.

The water content on a drying scanning curve at a specific soil suction ψ is subsequently scaled using the methodology established by Scott et al. (1983). This scaling process is initiated from the original drying curve, with the reversal point denoted as $(\theta_\Delta, \psi_\Delta)$, as illustrated in the work of Šimunek et al. (2012).

$$\theta_\psi = \theta_r^{ds} + \beta[\theta^d(\psi) - \theta_r^d]$$

where = $\theta^d(\psi)$ = volumetric water content on the initial drying curve at soil suction (ψ); β = parameter related to the reversal point, $\beta = \frac{\theta_\Delta - \theta_r^d}{\theta^d(\psi) - \theta_r^d}$; θ_r^{ds} = residual volumetric water content for a drying scanning curve, $\theta_r^{ds} = \theta_s - \beta(\theta_s^d - \theta_r^d)$ and θ_s = volumetric water content for a scanning curve at zero soil suction, $\theta_s = \frac{\theta_s^d - (\theta_s^d - \theta_\Delta)}{1 + R(\theta_s^d - \theta_\Delta)}$, where $R = \frac{1}{\theta_s^d - \theta_s^w} - \frac{1}{\theta_s^d - \theta_r^w}$.

The wetting scanning curve at soil suction, ψ, is similarly derived from the primary wetting curve, particularly when the reversal point $(\theta_\Delta, \psi_\Delta)$ is specified, as demonstrated by Šimunek et al. (2012).

$$\theta_\psi = \theta_r^{ws} + \gamma[\theta^w(\psi) - \theta_r^w]$$

Where θ_r^{ws} = residual volumetric water content for the wetting scanning curve, $\theta_r^{ws} = \theta_s - \gamma(\theta_s^w - \theta_r^w)$; $\theta^w(\psi)$ = volumetric water content on the main wetting curve at the soil suction, ψ; and γ = parameter related to the reversal point, $\gamma = \frac{\theta_\Delta - \theta^s}{\theta^w(\psi) - \theta_s^w}$.

Certain limitations are applied to the hysteresis model to decrease the quantity of model parameters as outlined below.

$$\theta_r^d = \theta_r^w = \theta_r$$

If the level of air entrapment is minimal, then an additional limitation exists.

$$\theta_s^d = \theta_s^w$$

Notably, Equation ($\theta_s^d = \theta_s^w$) assumes identical saturated water content for drying/wetting, which neglects air entrapment effects. This simplification may underestimate hysteresis in shallow layers but was necessary for model stability.

Furthermore, it is essential to establish the subsequent constraint to delineate a nonhysteretic conductivity function, $k(\theta)$:

$$n^d = n^w = n$$

Kool and Parker (1987) elucidate that the limitation expressed in Equation ($n^d = n^w = n$) diminishes the adaptability of the hysteresis model in accurately representing soil water retention (SWR) behavior, a phenomenon that is evidenced by the simulation outcomes discussed in this study. The hydraulic

conductivity function, denoted as $k(\theta)$, was formulated by Mualem in 1976 and is characterized as follows.

$$k(S_e) = k_{sat} S_e^{0.5} \left[1 - \left(1 - S_e^{\frac{1}{m}}\right)^m\right]^2$$

where k_{sat} = saturated hydraulic conductivity.

The model developed by Kool and Parker in 1987 incorporates eight parameters $(\theta_s^d, \theta_s^w, \theta_r^d, \theta_r^w, \alpha^d, \alpha^w, n^d \text{ and } n^w)$ to effectively characterize the hysteretic soil water retention curve (SWRC). This model considers the influences of both capillary and air-entrapment hysteresis on the retention characteristics of soil. Within the limitations imposed by equations ($\theta_r^d = \theta_r^w = \theta_r$) and ($n^d = n^w = n$), the hydraulic hysteretic behavior is characterized by six parameters: $(\theta_s^d, \theta_s^w, \theta_r, \alpha^d, \alpha^w \text{ and } n)$. In contrast, the model proposed by Kool and Parker (1987) employs five parameters $(\theta_s^d, \theta_r, \alpha^d, \alpha^w \text{ and } n)$ to define the soil water retention curve (SWRC) while considering only capillary hysteresis.

The parameters $(\theta_s^d, \theta_r, \alpha^d \text{ and } n)$ were derived by calibrating the observed initial drying curve through the equation $S_e = \frac{\theta - \theta_r^d}{\theta_s^d - \theta_r^d} = \left[1 + (\alpha^d \psi^d)^{n^d}\right]^{-m^d}$.

The parameters $(\theta_s^w \text{ and } \alpha^w)$ were derived by calibrating the observed primary wetting curve through the equation $S_e = \frac{\theta - \theta_r^w}{\theta_s^w - \theta_r^w} = \left[1 + (\alpha^w \psi^w)^{n^w}\right]^{-m^w}$.

The hysteresis model was integrated into the HYDRUS software, as demonstrated by Šimunek et al. (2012).

3.0 RESULTS AND DISCUSSION

3.1 Evaluating Hydraulic Hysteresis in 2D Unsaturated Flow Using the Kool and Parker Model

The Kool and Parker (1987) model was applied using the HYDRUS software, as detailed by Šimunek et al. (2012). This software facilitated the simulation of two-dimensional (2D) unsaturated flow scenarios. Additionally, to assess the significance of hydraulic hysteresis, the initial drying curve was incorporated into the numerical model to replicate the same flow issues where hydraulic hysteresis was not taken into account.

3.2 HYDRUS Evaluation for Unsaturated Flow Using Soil Column and Axis-Translation

Prior to evaluating the legitimacy of the constitutive model for soil water retention curves (SWRC) established by Kool and Parker in 1987, it is essential to investigate the numerical frameworks, such as HYDRUS, that are designed to address the challenges associated with unsaturated flow. In pursuit of this objective, a soil column test was implemented to evaluate the numerical code.

One of the two indirect approaches for assessing the hydraulic conductivity function, commonly known as the k-function, involves the utilization of the water retention curve (WRC). In laboratory settings, pressure plate tests, as outlined in ASTM D2325-68 (ASTM 1997), are frequently employed to determine the WRC. This method allows for the application of suction to a soil sample by maintaining a state of zero pore-pressure while simultaneously introducing positive pore-air pressure. Consequently, the level of suction exerted on the soil specimen can be adjusted by varying the air pressure applied to the sample. This technique is known as the axis-translation method. This section primarily addresses the efficacy of the numerical framework in modeling the unsaturated flow problem. The water retention curve of clay loam soil was obtained from pressure plate test (Figure.2). Figure 2 presents the experimental WRC for clay loam, determined via axis-translation (ASTM D2325) under controlled drying-wetting cycles. The fitted van Genuchten parameters (Table 1) were derived from nonlinear regression of this dataset, with α and n optimized separately for the initial drying (IDC) and main wetting curves (MWC) to capture hysteresis. The soil intended for the experiment was collected from a depth of two meters in the lands in the western part of Kermanshah city.

Soil sampling followed ASTM D4220-95 standards, with three replicate cores extracted per location. Particle size distribution (ASTM D6913) classified the soil as clay loam, consistent with USDA texture classifications. Prior to testing, samples were oven-dried at 105°C for 24 hours to remove residual moisture.

Consequently, the initially drying curve was incorporated into the models solely to simulate unsaturated flow, while the influence of hydraulic hysteresis wasn't taken into account. The height of the soil column was 65 cm. At the outset, the entire soil column was completely saturated. The established boundary conditions were as follows: first, the infiltration rate at the top was set to 0.0; second, the pressure head at the base varied from 65 cm to 0 cm; and third, both lateral sides were rendered impermeable to both water and air.

The no-flux top boundary simulates a sealed column preventing evaporation, while the seepage face at the base represents a free-draining outlet. Lateral impermeability mimics rigid column walls, consistent with axis-translation apparatus constraints [ASTM D2325].

These boundary conditions—fully saturated initial state and no-flux upper surface—represent controlled experimental scenarios to isolate hysteresis effects on drainage dynamics. While field conditions typically involve unsaturated initial states and transient surface fluxes (e.g., rainfall, evaporation), these simplifications enable mechanistic validation of the Kool-Parker model under reproducible settings, analogous to laboratory column studies [14, 40]. Subsequent research should extend this framework to field-relevant boundary conditions.

The HYDRUS-2D simulations utilized a finite element mesh consisting of 9,914 nodes and 19,496 2D elements to discretize the soil domain. Temporal discretization employed an adaptive time-stepping scheme, starting from an initial time step of 0.01 minutes (0.6 seconds) and reaching a maximum time step of 66.67 minutes at later stages, with a minimum step constraint of 10 seconds imposed to ensure numerical stability. This mesh density and time-step criteria were selected to balance computational efficiency with the resolution required for accurate simulation of the transient drainage processes and to maintain numerical convergence throughout the simulation period (0 to 300 minutes).

Mesh sensitivity analysis confirmed that further refinement (>22,000 elements) altered suction predictions by <1%. The hysteresis algorithm was activated using the 'Hysteresis'

module in HYDRUS, with scanning parameters initialized via the Parker-Lenhard scaling approach [40]. The adaptive time step ensured Courant numbers <0.3, critical for stability during rapid drainage onset near the seepage face.

Table 1 Material properties and SWRC parameters of clay loam soil

Saturated Hydraulic Conductivity (k_{sat}(m/s))	4.01×10^{-6}
Density of Solid Phase ($\rho_s\ kg/m^3$)	1.18×10^{3}
Density of Water ($\rho_w\ kg/m^3$)	1×10^{3}
Density of Air ($\rho_a\ kg/m^3$)	1.20
Gravity ($g\ \ m/s^2$)	9.81
Dynamic Fluid Viscosity of Water ($\mu_w\ Pa.s$)	1×10^{-3}
Dynamic Fluid Viscosity of Air ($\mu_a\ Pa.s$)	1.8×10^{-5}
Porosity ($\eta_0\ cm^3/cm^3$)	0.521
Residual Volumetric Water Content ($\theta_r\ cm^3/cm^3$)	0.088
Saturated Volumetric Water Content ($\theta_s\ cm^3/cm^3$)	0.521
n_d for Initial Drying Curve	1.2878
$\alpha_d(cm^{-1})$ for Initial Drying Curve	0.0157
n_w for Main Wetting Curve	1.2878
$\alpha_w(cm^{-1})$ for Main Wetting Curve	0.0314
Scanning Parameter (suction ratio) (cm)	2.000003131

The parameters related to the materials and model used in the HYDRUS-2D simulation are detailed in Table 1.

The HYDRUS-2D model was parameterized using soil hydraulic properties determined from laboratory pressure plate tests (ASTM D2325-68; Figure 2, Table 1). Numerical calibration was achieved through internal validation against a 1D soil column drainage scenario within HYDRUS-2D, ensuring consistency with fundamental unsaturated flow principles. No independent experimental data were used to validate transient suction or volumetric water content dynamics; instead, model performance was assessed via statistical metrics (R^2, RMSE) and regression fits comparing hysteresis-inclusive and hysteresis-ignoring scenarios.

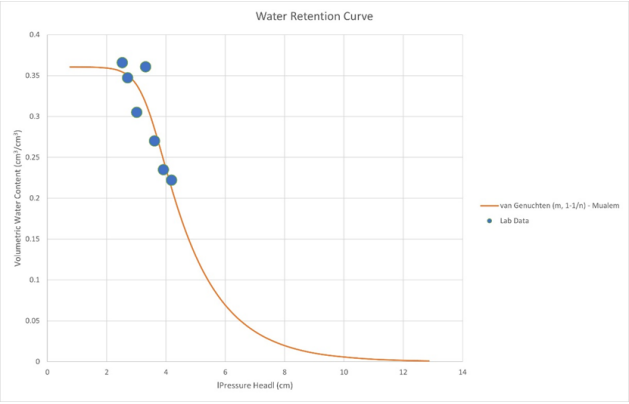

Figure 2 Water retention curve (WRC) of the clay loam soil selected for the test

3.3 Suction Trends and Drainage Dynamics in Clay Loam Soil: Impacts of Hysteresis Omission

The Hydrus-2D simulation modeled drainage behavior in a fully saturated Clay Loam soil column, employing van-Genuchten parameters typical for USDA classifications, with boundary conditions that included no-flux upper and lateral boundaries (0.0 cm/h flux and zero air pressure) and a seepage face at the bottom boundary under zero air pressure. The analysis of the simulation data provided critical insights into suction trends, drainage dynamics, and inherent model limitations. Three observation points at varying depths (Point 1: Z=51.17cm, point 2: Z=33.8cm, and point 3: Z=15.14cm) demonstrate distinct suction behaviors over time (Figure.3). Figure 3 illustrates the mesh geometry and nodal distribution, confirming sufficient resolution (9,914 nodes) near observation points to resolve depth-dependent gradients. The Z-coordinates explicitly reference distance from the bottom boundary, ensuring proximity-driven dynamics are mechanistically interpreted. When plotted on a semi-logarithmic axis, point 1, positioned closest to the upper boundary, exhibited the steepest suction increase, reaching −29.18cm at 300 minutes. In contrast, Points 2 and 3 showed slower development (−20.30cm and −10.90cm, respectively), highlighting vertical variability in drainage dynamics linked to depth-dependent desaturation (Figure.4). Figure 4 explicitly illustrates the depth-dependent acceleration of suction development, where Point 1 (deepest) exhibits the steepest initial slope, signifying rapid drainage near the seepage face. The convergence of all curves towards near-steady-state suction values by 300 minutes highlights the progression from transient to equilibrium drainage conditions. The exponential decay model fits (solid lines) quantitatively confirm faster suction increase rates (higher k values) with increasing depth.

Further analysis of suction change rates identified three phases. During the early transient phase (0–2 minutes), suction declined rapidly (e.g., Point 1: −0.569cm/min to −1.083cm/min). The intermediate phase (2–50 minutes) saw decreasing rates (Point 1: −0.215cm/min to −7.279cm/min), transitioning to near-steady-state conditions (dS/dt→0) after 50 minutes. By 300 minutes, Point 1's suction stabilized at −29.18cm with a minimal rate of −0.003cm/min. Exponential decay models ($S(t)=S_0-A(1-e^{-kt})$) fit the data robustly ($R^2>0.9$), with shallower points exhibiting faster decay rates (Point 1: A=29.2, k=0.025min^{-1}; Point 2: A=20.3, k=0.018min^{-1}; Point 3: A=10.9, k=0.012min^{-1}).

The omission of hysteresis in the model introduces limitations. By assuming a single retention curve, suction during drainage may be overestimated, as hysteresis in clay loam soils can reduce suction by 10–20% during drying cycles, as suggested by prior studies. [33, 43]. Consequently, simulated results represent a "best-case" drainage scenario without accounting for wetting reversals.

Methodologically, the simulation utilized fully saturated clay loam (USDA classification) with no-flux boundaries at the top and sides, and a zero-pressure boundary at the bottom. The 300-minute duration ensured near-steady-state conditions. Key takeaways include: (1) suction magnitude correlates inversely with depth, (2) exponential models effectively describe suction dynamics, and (3) hysteresis neglect may overpredict suction by 10–20% in real-world cyclic conditions. These findings

underscore the importance of depth-specific analysis and model limitations in interpreting drainage behavior.

Three observation points at varying depths (51.17 cm, 33.8 cm, and 15.14 cm) tracked volumetric water content (VWC) over 300 minutes (Figure.5). Figure 5 demonstrates the inverse relationship between depth and drainage rate. Point 1 (deepest) shows the most rapid VWC decline and lowest equilibrium moisture, driven by proximity to the drainage boundary and stronger gravitational gradients. Conversely, Point 3 (shallowest) retains significantly higher VWC due to dominant capillary forces, evidenced by its slower decay rate and flatter slope. The exponential decay fits quantify these depth-stratified drainage dynamics, with shallower layers exhibiting smaller decay constants (k).

All points exhibited gradual VWC declines due to gravitational drainage, with distinct depth-dependent trends. Observation Point 1 (deepest (The deepest in relation to the bottom has been specified) at 51.17 cm) showed the most rapid drainage, decreasing from 0.521 to 0.4919 VWC (Δ = -0.0291) at an average rate of -9.7×10^{-5} min^{-1}, reaching equilibrium around 150 minutes. Point 2 (33.8 cm depth) displayed intermediate behavior, with a final VWC of 0.5015 (Δ = -0.0195) and a rate of -6.5×10^{-5} min^{-1}, stabilizing near 200 minutes. Point 3 (shallowest at 15.14 cm) drained slowest, ending at 0.5116 VWC (Δ = -0.0094) with a rate of -3.1×10^{-5} min^{-1} and approaching equilibrium after ~250 minutes.

A dedicated analysis of spatial differences revealed that drainage rates and equilibrium VWC correlated strongly with depth. Deeper zones experienced faster initial drainage due to proximity to the seepage face and stronger gravitational forces. Shallower regions retained higher moisture due to capillary retention and reduced gravitational influence, while intermediate depths (Point 2) exhibited transitional behavior.

The study concludes that the simulation effectively captures depth-dependent drainage dynamics in homogeneous Clay Loam. However, ignoring hysteresis in the retention curve introduces notable biases: simulated drainage rates may be overestimated due to the absence of pore-water retention effects during drying cycles, and equilibrium VWC values are likely underestimated. These simplifications are acceptable for theoretical analyses.

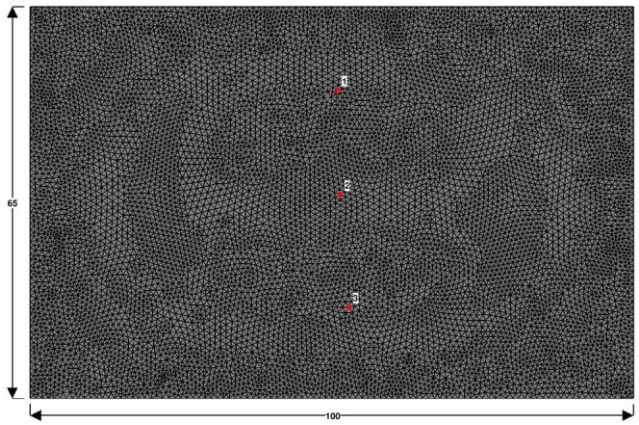

Figure 3 HYDRUS-2D Mesh, and Observation Nodes

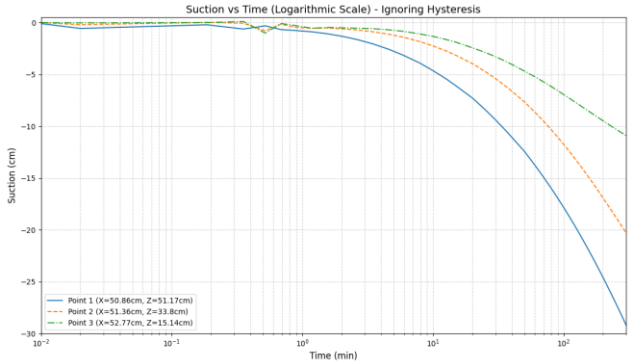

Figure 4 Suction vs Time (Ignoring Hysteresis)

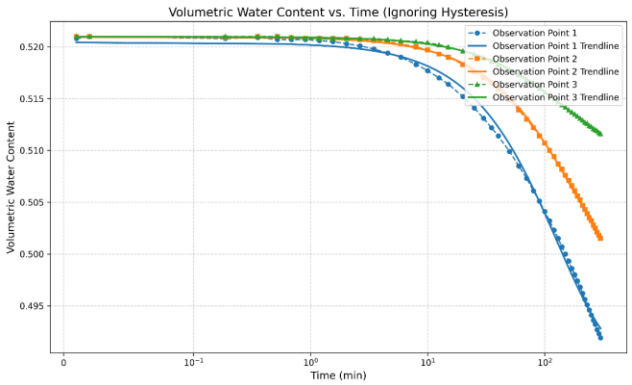

Figure 5 Volumetric Water Content vs Time (Ignoring Hysteresis)

3.4 Numerical Study of Hysteresis Effects on Suction and Volumetric Water Content Dynamics

This study investigates hysteresis effects and time-dependent suction trends in a draining clay loam soil column simulated via Hydrus-2D (the parameters of the Kool and Parker (1987) model are presented in Table 1), utilizing Clay Loam soil (with physical properties detailed in Table 1) as the experimental. The Clay Loam soil column was considered completely saturated. The boundary conditions were defined in the following manner: (1) at the upper boundary, the flux was set to 0.0 cm/h; (2) at both lateral boundaries, the flux remained at 0.0 cm/h; and (3) The air pressure was also maintained at 0, while HYDRUS–2D operates under the assumption of a consistent pressure head of zero across the saturated (active) section of the seepage face, facilitating the outflow of water from the saturated region of the domain at the bottom boundary.

The analysis focuses on three observation points at varying depths (Point 1: 51.17 cm, point 2: 33.8 cm, point 3: 15.14 cm), revealing distinct suction behaviors governed by vertical positioning and soil hydraulic properties (Figure.6). Figure 6 explicitly demonstrates how hysteresis modulates suction dynamics across depths. The slower suction development at shallower depths (Point 3) contrasts with rapid changes at Point 1, illustrating hysteresis-induced delays in drainage propagation. Divergence between depth-specific curves highlights path-dependent retention behavior, where soil 'remembers' prior wetting states—evidenced by non-parallel trends during drainage.

Suction (negative pressure head) increased with depth, aligning with drainage initiation at the bottom boundary (seepage face). At 300 minutes, point 1 exhibited the most negative suction (−28.726 cm), followed by Point 2 (−20.002 cm) and Point 3 (−10.805 cm). A pronounced response lag was observed: deeper layers desaturated faster, with Point 1 reaching −4.329 cm at 10 minutes, while Point 3 lagged at −1.316 cm. This reflects upward propagation of drainage from the seepage face, driven by steeper hydraulic gradients near the base.

Hysteresis effects were quantified through loop width and area. The maximum suction divergence between Points 1 and 3 at 300 minutes was 17.921 cm. Using the trapezoidal rule, the cumulative hysteresis loop area between Points 1 and 3 was calculated as 1,245 cm·min, underscoring depth-dependent retention curve variability. Regression analyses confirmed strong power-law relationships between suction (h) and time (t) for all points, with high R^2 values (Point 1: 0.992; Point 2: 0.989; Point 3: 0.985). The equations—h=−0.874·t^0.613 (Point 1), h=−0.532·t^0.589 (Point 2), and h=−0.298·t^0.562 (Point 3)—highlight faster suction development in deeper layers. Corresponding average suction rates (dh/dt) decreased with proximity to the surface: −0.095 cm/min (Point 1), −0.067 cm/min (Point 2), and −0.036 cm/min (Point 3).

Spatially, suction magnitude and rate inversely correlated with depth due to proximity to the drainage boundary and hydraulic gradient intensity. The Hydrus-2D model configuration—zero flux at top/lateral boundaries and a seepage face at the bottom—explained the unidirectional drainage pattern. Clay loam's low hydraulic conductivity further delayed suction equilibration, amplifying hysteresis.

Interpretations attribute divergent suction evolution to boundary proximity and soil retention hysteresis. Point 1, near the seepage face, experienced immediate drainage, while Point 3 responded later as drainage propagated upward. The model's hysteresis algorithm captured non-unique suction-moisture relationships, where deeper layers retained higher suction due to irreversible pore drainage.

In conclusion, vertical positioning critically governs suction dynamics in clay loam, validated by hysteresis metrics and regression models. Boundary conditions and soil properties collectively drive depth-dependent trends, enhancing mechanistic understanding of hysteresis in unsaturated flow simulations. These insights underscore the importance of incorporating hysteresis algorithms in hydrological models for accurate prediction of soil-water interactions.

This study investigates hysteresis effects in volumetric water content over time across different soil depths, emphasizing disparities in drainage rates influenced by gravitational gradients and path-dependent retention. Observations from three points—varying in depth from 15.14 cm (shallowest, point 3) to 51.17 cm (deepest, point 1)—revealed distinct drainage behaviors (Figure.7). Figure 7 visualizes hysteresis-driven moisture retention, particularly in shallow zones (Point 3). The flatter VWC slope at Point 3 versus steeper declines at Point 1 confirms reduced drainage efficiency due to capillary hysteresis and air entrapment. Exponential decay constants (k) quantitatively reflect this: k=0.0012 min^{-1} (Point 3) versus 0.0035 min^{-1} (Point 1) aligns with theoretical hysteresis models where pore connectivity loss during drying slows drainage. The deepest layer exhibited the fastest drainage, with volumetric water content decreasing from 0.521 to 0.4924, attributed to stronger gravitational forces. In contrast, the shallowest layer retained moisture longer (0.521 to 0.5117), a phenomenon linked to hysteresis, where soil moisture retention depends on historical saturation states. Exponential decay models quantified these trends, with decay constants (k) ranging from 0.0035 min^{-1} (Point 1) to 0.0012 min^{-1} (Point 3), supported by high R^2 values (0.95–0.98) and statistically significant differences confirmed via ANOVA ($p < 0.01$).

Hysteresis effects were particularly pronounced in shallow layers, where reduced hydraulic conductivity during drying cycles slowed drainage. This aligns with the Parker-Lenhard model, a theoretical framework describing how air entrapment in fine-textured soils (e.g., clay loam) impedes water movement. The model's predictions matched observed behaviors, such as prolonged retention in upper layers due to residual air pressure under zero-flux boundary conditions. Confidence intervals for decay rates further highlighted overlapping trends in mid-to-upper layers (Points 2 and 3), suggesting comparable hysteresis impacts despite depth variations.

The Hydrus-2D simulation—a computational tool for modeling water flow in unsaturated soils—replicated these dynamics under controlled conditions: clay loam soil, fully saturated initial states, and boundary constraints mimicking natural drainage. Geometric layering in the simulation reinforced depth-dependent patterns, with slower drainage at shallower depths reflecting both gravitational limitations and hysteresis-induced conductivity losses. Minor anomalies, such as transient sensor noise at Point 1, were deemed negligible compared to the broader trends.

Findings corroborate existing literature, including decay rates for clay loam (0.001–0.004 min^{-1}) and theoretical models like Scott-Klug, which attribute "memory effects" in shallow layers to historical saturation states. The study underscores hysteresis as a critical factor in hydrological modeling, particularly in stratified soils where path-dependent retention governs water redistribution.

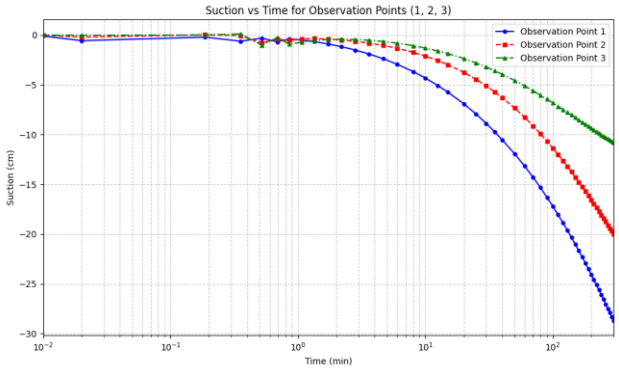

Figure 6 Suction vs Time (Considering Hysteresis)

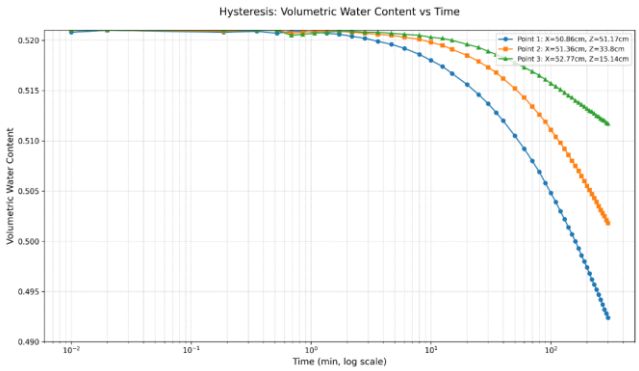

Figure 7 Volumetric Water Content vs Time (Considering Hysteresis)

3.5 Comparative Analysis of Hysteresis-Inclusive vs. Hysteresis-Ignoring Models on Soil Suction and Volumetric Water Content: Depth-Dependent and Temporal Impacts

The study compares suction data with and without accounting for hysteresis to evaluate its impact on soil behavior. Mismatched time points between datasets (e.g., 0.9033 min vs. 0.8533 min) were resolved using linear interpolation, ensuring alignment for direct comparison. Analysis revealed consistent positive differences (ΔSuction = Hysteresis Suction − Ignoring Hysteresis Suction) across observation points, indicating that hysteresis reduces suction decline. For instance, at Observation Point 1 (depth Z=51.17 cm), ΔSuction increased from +0.314 cm (6.76%) at 10.0 min to +0.634 cm (3.55%) at 100.0 min and +0.456 cm (1.56%) at 300.0 min. These results support the hypothesis that hysteresis causes slower suction decline, with differences amplifying over time, particularly during transient phases (150–200 min) (Figure 8). Maximum deviations (e.g., +0.76 cm at 150 min for Point 1, representing 3.51% of the baseline suction) aligned with critical suction thresholds during transient drainage phases.

Statistical metrics further validated these trends. The statistical robustness of the reported RMSE and p-values is underpinned by high-resolution temporal data derived from HYDRUS-2D simulations. For each observation point (Points 1–3), suction and volumetric water content (VWC) dynamics were recorded at 50 discrete time steps under hysteresis-ignoring conditions (Figures 4–5) and 51-time steps under hysteresis-inclusive conditions (Figures 6–7). This yielded 50–51 paired data points per depth for comparative analyses (e.g., ΔSuction, ΔVWC). Regression models (e.g., exponential decay, power-law) and hypothesis testing (paired t-tests, ANOVA) were thus applied to datasets of size n=50 (ignoring hysteresis) and n=51 (considering hysteresis) per depth. Figure 8 visually synthesizes these statistical trends, demonstrating that hysteresis-inclusive models (solid lines) consistently yield higher suction values (i.e., less negative) than hysteresis-ignoring simulations (dashed lines) across all depths. Crucially, the divergence between models widens most significantly at deeper layers (Point 1), particularly during transient drainage phases (0–200 min), aligning with the RMSE depth-dependency. This divergence underscores hysteresis-induced delays in drainage progression, where the retention of antecedent moisture slows suction development—especially near the seepage face. The sample sizes ensure statistical power, with RMSE values reflecting deviations across all simulated time steps and p-values (<0.05) confirming significance against rigorous thresholds.

The Root Mean Square Error (RMSE) increased with depth, reaching 0.48 cm at Point 1 (Z=51.17 cm), compared to 0.21 cm at the shallowest point (Z=15.14 cm), highlighting stronger hysteresis effects in deeper soil layers. When expressed as a percentage of mean absolute suction, RMSE values were 4.0% at Point 1 and 4.2% at Point 3. High R^2 values (>0.97) confirmed strong correlations between models, though systematic deviations persisted due to hysteresis.

Spatial sensitivity analysis underscored depth-dependent variations. At 300 min, ΔSuction was most pronounced at Point 1 (+0.456 cm, 1.56%), followed by Point 2 (Z=33.80 cm; +0.295 cm, 1.45%) and Point 3 (Z=15.14 cm; +0.099 cm, 0.91%). This pattern suggests deeper layers experience delayed drainage dynamics and higher moisture retention, amplifying hysteresis impacts.

The findings validate that hysteresis-inclusive models yield less negative suction values, mitigating overestimations of suction decline. This has critical implications for scenarios like slope stability and irrigation planning, where ignoring hysteresis could lead to erroneous predictions.

The study analyzed the impact of hysteresis on soil moisture dynamics by comparing volumetric water content (VWC) between models incorporating hysteresis and those ignoring it. Linear interpolation was applied to align time points across datasets, focusing on exact matching times post-interpolation at three observation points (Point 1: ~51 cm depth; Point 2: ~34 cm; Point 3: ~15 cm). Differences in VWC (ΔVWC) were calculated as Hysteresis VWC – Ignoring Hysteresis VWC, where negative values indicate lower drainage in the hysteresis model (Figure 9).

Quantitatively, paired t-tests confirmed statistically significant differences ($p < 0.05$) at all points (point one: $p = 1.16\times10^{-16}$, point two: $p = 2.4\times10^{-8}$, point three: $p = 0.0026$), with the strongest effects at the shallowest depth (Point 3). At Point 3, ΔVWC reached -0.0041 (0.79% of baseline VWC) within 10 minutes, reflecting early and pronounced discrepancies. Deeper layers (Points 1 and 2) exhibited smaller differences, peaking later: Point 1 showed a maximum ΔVWC of -0.0023 (0.47%) at 300 minutes, while Point 2 reached -0.0017 (0.34%) at the same time. These results highlight spatial and temporal variability, with hysteresis retaining slightly more water long-term in deeper layers but causing delayed drainage in shallow soils.

Qualitatively, hysteresis consistently slowed drainage across all observation points. Figure 9 directly contrasts VWC evolution, revealing that hysteresis-inclusive models (solid lines) retain higher moisture than hysteresis-ignoring simulations (dashed lines) throughout drainage. The largest discrepancies occur in shallow soils (Point 3), where hysteresis preserves 0.79% more VWC within 10 minutes due to capillary retention. Conversely, deeper layers (Point 1) exhibit delayed but sustained moisture retention (ΔVWC = -0.47% at 300 min), highlighting hysteresis-driven 'memory effects' that decouple drainage rates from instantaneous hydraulic gradients. These visual trends quantitatively validate hysteresis as a non-negligible modulator of field-scale water storage. Shallow layers (Point 3) experienced the largest discrepancies, with ΔVWC magnitudes twice as high as deeper layers during early phases (0–10 minutes). This was attributed to proximity to

surface boundary conditions like evaporation. In contrast, deeper layers (Points 1–2) showed gradual divergence during late phases (200–300 minutes), driven by stable moisture gradients. The wetting phase influence, though not explicitly captured in outputs, likely buffered drainage rates through hysteresis parameters during transient cycles.

Key findings emphasize that hysteresis reduces drainage rates most notably in shallow soils, with maximum differences occurring early in surface layers and late in deeper layers. For models in dynamic environments, such as agricultural fields, incorporating hysteresis parameters is critical to avoid underestimating near-surface water retention.

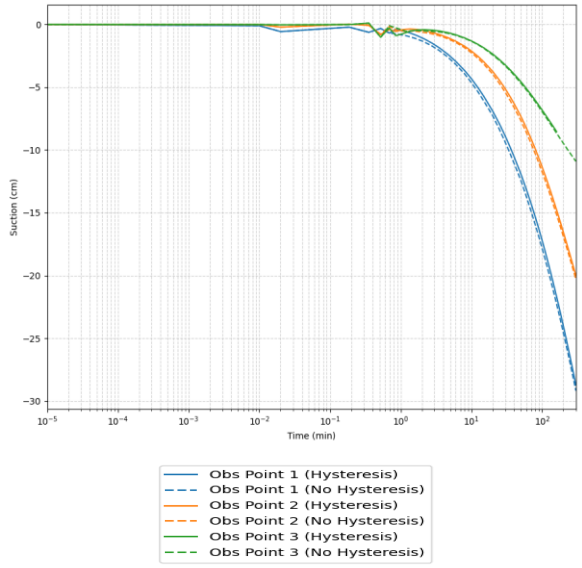

Figure 8 Suction vs Time (Ignoring vs Considering Hysteresis)

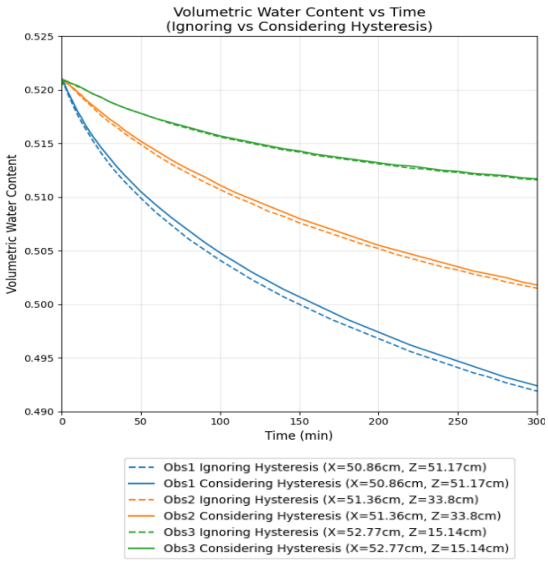

Figure 9 Volumetric Water Content vs Time (Ignoring vs Considering Hysteresis)

4.0 CONCLUSION

This study elucidates the interplay between depth-dependent drainage dynamics and hydraulic hysteresis in unsaturated flow through a clay loam soil column, employing Hydrus-2D simulations grounded in the Kool and Parker (1987) constitutive model. The findings underscore critical theoretical and modeling insights, emphasizing the necessity of integrating vertical stratification and hysteresis effects for robust hydrological simulations.

Vertical positioning within the soil column governs suction and volumetric water content (VWC) evolution. Deeper layers, proximate to the seepage face, exhibited faster drainage rates and steeper suction gradients due to intensified gravitational forces and hydraulic gradients. Conversely, shallow layers retained higher moisture levels, driven by capillary retention and reduced gravitational influence. Exponential decay and power-law models effectively captured these trends, with shallower depths demonstrating prolonged equilibration times. The simulations highlighted the unidirectional drainage pattern under no-flux lateral and upper boundaries, reinforcing the role of boundary conditions in shaping vertical moisture redistribution.

Neglecting hydraulic hysteresis introduced systematic biases, overestimating suction magnitudes and underestimating equilibrium VWC. Hysteresis-inclusive models revealed slower suction decline and delayed drainage, particularly in shallow layers, where historical saturation states and pore-water retention effects dominated. These path-dependent behaviors were amplified in fine-textured soils, aligning with theoretical frameworks that attribute hysteresis to air entrapment and irreversible pore drainage. Statistical validation confirmed stronger hysteresis effects in deeper layers during transient phases, though shallow layers exhibited the most pronounced discrepancies in VWC retention.

The study advances hydrological modeling by demonstrating the necessity of hysteresis algorithms to capture non-unique suction-moisture relationships. The integration of depth-specific analysis and hysteresis parameters mitigates overestimations in drainage rates and suction decline, critical for simulating cyclic wetting-drying scenarios. Furthermore, the validated exponential and power-law relationships provide mechanistic insights into time-dependent suction dynamics, emphasizing the interplay between soil hydraulic properties, boundary conditions, and retention curve variability.

In conclusion, this work bridges theoretical and computational hydrology by quantifying the dual influences of vertical stratification and hydraulic hysteresis. Future models must prioritize these factors to enhance predictive accuracy in unsaturated flow simulations, particularly for heterogeneous soils under dynamic hydrological regimes.

Acknowledgement

This project was self-funded by the author. However, I extend my sincere gratitude to Razi University for providing access to specific facilities/resources, e.g., laboratories, libraries, equipment, and administrative support. I am deeply thankful to my supervisor, Dr. Hassan Sharafi, for their invaluable mentorship, expert guidance, and constructive feedback throughout this project.

Conflict of Interest

The author(s) declare(s) that there is no conflict of interest regarding the publication of this paper

References

[1] Al-Soudany, K. Y. H., Fattah, M. Y., & Rahil, F. H. 2024. Enhancement of Expansive Soil Properties by Water Treatment Sludge Ash in Landfill Liners. *Civil Engineering Journa*l, 10(11): 3508–3530. DOI: https://doi.org/10.28991/cej-2024-010-11-04.

[2] Baum, R. L., Godt, J. W., & Savage, W. Z. 2010. Estimating the timing and location of shallow rainfall-induced landslides using a model for transient, unsaturated infiltration. *Journal of Geophysical Research: Earth Surface,* 115(F3): 1-26. DOI: https://doi.org/10.1029/2009JF001321.

[3] Beriozkin, A., & Mualem, Y. 2018. Comparative analysis of the apparent saturation hysteresis approach and the domain theory of hysteresis in respect of prediction of scanning curves and air entrapment. *Advances in Water Resources*, 115: 253-263. DOI: https://doi.org/10.1016/j.advwatres.2018.01.016.

[4] Beville, S. H., Mirus, B. B., Ebel, B. A., Mader, G. G., & Loague, K. 2010. Using simulated hydrologic response to revisit the 1973 Lerida Court landslide. *Environmental Earth Sciences,* 61(6): 1249-1257. DOI: https://doi.org/10.1007/s12665-010-0448-z.

[5] Bikerman, J. J. 1974. Capillary Attraction and Hysteresis of Wetting. *The Journal of Adhesion*, 6(4): 331-336. DOI: https://doi.org/10.1080/00218467408075036.

[6] Bond, W. J., & Collis-George, N. 1981. Ponded infiltration into simple soil systems: 1. The saturation and transition zones in the moisture content profiles. *Soil Science,* 131(4): 202-209. DOI: https://doi.org/10.1097/00010694-198104000-00002.

[7] Cihan, A., Birkholzer, J., Illangasekare, T. H., & Zhou, Q. 2014. A modeling approach to represent hysteresis in capillary pressure-saturation relationship based on fluid connectivity in void space. *Water Resources Research*, 50(1): 119-131. DOI: https://doi.org/10.1002/2013WR014280.

[8] Chen, P., Mirus, B., Lu, N., & Godt, J. W. 2017. Effect of hydraulic hysteresis on stability of infinite slopes under steady infiltration. Journal of Geotechnical and Geoenvironmental Engineering, 143(9): 04017041. DOI: https://doi.org/10.1061/(ASCE)GT.1943-5606.0001724.

[9] Chen, P., & Wei, C. 2016. Numerical procedure for simulating the two phase flow in unsaturated soils with hydraulic hysteresis. International Journal of Geomechanics, 16(1): 04015030. DOI: https://doi.org/10.1061/(ASCE)GM.1943-5622.0000505.

[10] Chen, P., Wei, C., Liu, J., & Ma, T. 2013. Strength theory model of unsaturated soils with suction stress concept. Journal of Applied Mathematics, 2013: 1-11. DOI: https://doi.org/10.1155/2013/756854.

[11] Chen, P., Wei, C., & Ma, T. 2015. Analytical model of soil-water characteristics considering the effect of air entrapment. *International Journal of Geomechanics,* 15(6): 04014102. DOI: https://doi.org/10.1061/(ASCE)GM.1943-5622.0000462.

[12] Chen, P., & Wei, C. 2016. Numerical Procedure for Simulating the Two-Phase Flow in Unsaturated Soils with Hydraulic Hysteresis. *International Journal of Geomechanics,* 16(1): 04015030. DOI: https://doi.org/10.1061/(ASCE)GM.1943-5622.0000505.

[13] Ebel, B. A., Loague, K., & Borja, R. I. 2010. The impacts of hysteresis on variably saturated hydrologic response and slope failure. *Environmental Earth Sciences,* 61(6): 1215-1225. DOI: https://doi.org/10.1007/s12665-009-0445-2.

[14] Gillham, R. W., Klute, A., & Heermann, D. F. 1976. Hydraulic properties of a porous medium measurement and empirical representation. *Soil Science Society of America Journal*, 40(2): 203-207. DOI: https://doi.org/10.2136/sssaj1976.03615995004000020008x.

[15] Gillham, R. W., Klute, A., & Heermann, D. F. 1979. Measurement and numerical simulation of hysteretic flow in a heterogeneous porous medium. *Soil Science Society of America Journal,* 43(6): 1061-1067. DOI: https://doi.org/10.2136/sssaj1979.03615995004300060001x.

[16] Hoa, N. T., Gaudu, R., & Thirriot, C. 1977. Influence of hysteresis effect on transient flows in saturated-unsaturated porous media. *Water Resources Research,* 13(6): 992-996. DOI: https://doi.org/10.1029/WR013i006p00992.

[17] Huang, H.-C., Tan, Y.-C., Liu, C.-W., & Chen, C.-H. 2005. A novel hysteresis model in unsaturated soil. *Hydrological Processes*, 19(8): 1653-1665. DOI: https://doi.org/10.1002/hyp.5594.

[18] Jeong, S., Kim, Y., & Park, H. 2019. Influences of rainfall infiltration and hysteresis SWCC of unsaturated soil on settlement of shallow foundations. *Japanese Geotechnical Society Special Publication*, 7(2): 569-575. DOI: https://doi.org/10.3208/jgssp.v07.088.

[19] Kechavari, C., Soga, K., & Illangasekare, T. H. 2005. Two-dimensional laboratory simulation of LNAPL infiltration and redistribution in the vadose zone. *Journal of Contaminant Hydrology,* 76(Feb): 211-233. DOI: https://doi.org/10.1016/j.jconhyd.2004.09.001.

[20] Khalili, N., Habte, M. A., & Zargarbashi, S. 2008. A fully coupled flow deformation model for cyclic analysis of unsaturated soils including hydraulic and mechanical hysteresis. *Computers and Geotechnics,* 35(6): 872-889. DOI: https://doi.org/10.1016/j.compgeo.2008.08.003.

[21] Khoury, N., Brooks, R., Khoury, C., & Yada, D. 2012. Modeling resilient modulus hysteretic behavior with moisture variation. *International Journal of Geomechanics,* 12(5): 519-527. DOI: https://doi.org/10.1061/(ASCE)GM.1943-5622.0000140.

[22] Khoury, C. N., & Miller, G. A. 2012. Influence of hydraulic hysteresis on the shear strength of unsaturated soils and interfaces. *Geotechnical Testing Journal,* 35(1): 135-149. DOI: https://doi.org/10.1520/GTJ103616.

[23] Koestoer, R. H., Ligayanti, T., Kartohardjono, S., & Susanto, H. 2024. Down-streaming Small-Scale Green Ammonia to Nitrogen-Phosphorus Fertilizer Tablets for Rural Communities. *Emerging Science Journal,* 8(2): 625-643. DOI: https://doi.org/10.28991/esj-2024-08-02-016.

[24] Kool, J. B., & Parker, J. C. 1987. Development and evaluation of closed form expressions for hysteretic soil hydraulic properties. *Water Resources Research,* 23(1): 105-114. DOI: https://doi.org/10.1029/WR023i001p00105.

[25] Li, Y., Wu, P., Xia, Z., Yang, Q., Flores, G., Jiang, H., Kamon, M., & Yu, B. 2014. Changes in residual air saturation after thorough drainage processes in an air-water fine sandy medium. *Journal of Hydrology*, 519: 271-283. DOI: https://doi.org/10.1016/j.jhydrol.2014.07.019.

[26] Liu, C., & Muraleetharan, K. 2012. Coupled hydro-mechanical elastoplastic constitutive model for unsaturated sands and silts. I: Formulation. *International Journal of Geomechanics,* 12(3): 239-247. DOI: https://doi.org/10.1061/(ASCE)GM.1943-5622.0000146.

[27] Liu, J., Chen, P., & Li, W. 2018. Assessing Hydraulic Hysteresis Models to Characterize Unsaturated Flow Behavior under Drying and Wetting Conditions. *International Journal of Geomechanics*, 18(7): 04018084. DOI: https://doi.org/10.1061/(ASCE)GM.1943-5622.0001205.

[28] Liu, K., Vardon, P., Arnold, P., & Hicks, M. A. 2015. Effect of hysteresis on the stability of an embankment under transient seepage. IOP Conference Series: Earth and Environmental Science, 26: 012013. DOI: https://doi.org/10.1088/1755-1315/26/1/012013.

[29] Lu, N., Kaya, M., Collins, B. D., & Godt, J. W. 2013. Hysteresis of unsaturated hydrochemical properties of a silty soil. *Journal of Geotechnical and Geoenvironmental Engineering*, 139(3): 507-510. DOI: https://doi.org/10.1061/(ASCE)GT.1943-5606.0000786.

[30] Ma, T., Wei, C., Wei, H., & Li, W. 2016. Hydraulic and mechanical behavior of unsaturated silt: Experimental and theoretical characterization. *International Journal of Geomechanics,* 16(6): D4015007. DOI: https://doi.org/10.1061/(ASCE)GM.1943-5622.0000576.

[31] Min, T.-K., & Huy, P. T. 2010. A Soil-Water hysteresis model for unsaturated sands based on fuzzy set plasticity theory. *KSCE Journal of Civil Engineering*, 14(2): 165-172. DOI: https://doi.org/10.1007/s12205-010-0165-x.

[32] McCord, J. T., Stephens, D. B., & Wilson, J. L. 1991. Hysteresis and state-dependent anisotropy in modeling unsaturated hillslope hydrologic processes. *Water Resources Research,* 27(7): 1501-1518. DOI: https://doi.org/10.1029/91WR00880.

[33] Miller, G. A., Khoury, C. N., Muraleetharan, K. K., Liu, C., & Kibbey, T. C. G. 2008. Effects of soil skeleton deformations on hysteretic

soil water characteristic curves: Experiments and simulations. *Water Resources Research,* 44(5): W00C06. DOI: https://doi.org/10.1029/2007WR006492.

[34] Moore, N. W. 2011. Adhesion Hysteresis from Interdependent Capillary and Electrostatic Forces. *Langmuir,* 27(7): 3678-3684. DOI: https://doi.org/10.1021/la200043a.

[35] Morita, M. 1996. Numerical Methods for Three-dimensional Unsaturated Subsurface Flow. *Proceedings of Hydraulic Engineering,* 40: 437-442. DOI: https://doi.org/10.2208/prohe.40.437.

[36] Mualem, Y. 1976. A new model for predicting hydraulic conductivity of unsaturated porous media. *Water Resources Research,* 12(3): 513-522. DOI: https://doi.org/10.1029/WR012i003p00513.

[37] Mualem, Y., & Dagan, G. 1975. A dependent domain model of capillary hysteresis. *Water Resources Research,* 11(3): 452-460. DOI: https://doi.org/10.1029/WR011i003p00452.

[38] Muraleetharan, K., & Wei, C. 2001. *U-DYSCA2: Dynamic unsaturated soil analysis code for 2-dimensional problems*. Technical Report, School of Civil Engineering and Environmental Science, University of Oklahoma, Norman, OK.

[39] Muraleetharan, K. K., Liu, C., Wei, C., Kibbey, T. C. G., & Chen, L. 2009. An elastoplastic framework for coupling hydraulic and mechanical behavior of unsaturated soils. International Journal of Plasticity, 25(3): 473-490. DOI: https://doi.org/10.1016/j.ijplas.2008.04.001.

[40] Parker, J. C., & Lenhard, R. J. 1987. A model for hysteretic constitutive relations governing multiphase flow: 1. Saturation-pressure relations. *Water Resources Research,* 23(12): 2187-2196. DOI: https://doi.org/10.1029/WR023i012p02187.

[41] Parlange, J.-Y. 1976. Capillary hysteresis and relationship between drying and wetting curve. *Water Resources Research*, 12(2): 224-228. DOI: https://doi.org/10.1029/WR012i002p00224.

[42] Pasha, A. Y., Khoshghalb, A., & Khalili, N. 2017. Hysteretic model for the evolution of water retention curve with void ratio. *Journal of Engineering Mechanics,* 143(7): 04017030. DOI: https://doi.org/10.1061/(ASCE)EM.1943-7889.0001238.

[43] Pham, H. Q., Fredlund, D. G., & Barbour, S. L. 2003. A practical hysteresis model for the soil-water characteristic curve for soils with negligible volume change. *Géotechnique,* 53(2): 293-298. DOI: https://doi.org/10.1680/geot.2003.53.2.293.

[44] Pickens, J. F., & Gillham, R. W. 1980. Finite element analysis of solute transport under hysteretic unsaturated flow conditions. *Water Resources Research,* 16(6): 1071-1078. DOI: https://doi.org/10.1029/WR016i006p01071.

[45] Poulovassilis, A. 1970. The effect of the entrapped air on the hysteresis curves of a porous body and on its hydraulic conductivity. *Soil Science,* 109(3): 154-162. DOI: https://doi.org/10.1097/00010694-197003000-00003.

[46] Poulovassilis, A., & Childs, E. C. 1971. The hysteresis of pore water: the non-independence of domains. *Soil Science, 1*12(5): 301-312. DOI: https://doi.org/10.1097/00010694-197111000-00002.

[47] Rudiyanto, Sakai, M., Van Genuchten, M. Th., Alazba, A. A., Setiawan, B. I., & Minasny, B. 2015. A complete soil hydraulic model accounting for capillary and adsorptive water retention, capillary and film conductivity, and hysteresis. *Water Resources Research,* 51(11): 8757-8772. DOI: https://doi.org/10.1002/2015WR017703.

[48] Scarfone, R., Wheeler, S. J., & Lloret-Cabot, M. 2022. A hysteretic hydraulic constitutive model for unsaturated soils and application to capillary barrier systems. *Geomechanics for Energy and the Environment*, 30: 100224. DOI: https://doi.org/10.1016/j.gete.2020.100224.

[49] Scott, P. S., Farquhar, G. J., & Kouwen, N. 1983. Hysteresis effects on net infiltration. In *Proceedings of the National Conference on Advances in Infiltration*, 163-170. St. Joseph, MI: American Society of Agricultural and Biological Engineers.

[50] Seymour, R. M. 2000. Air entrapment and consolidation occurring with saturated hydraulic conductivity changes with intermittent wetting. *Irrigation Science,* 20(1): 9-14. DOI: https://doi.org/10.1007/PL00006716.

[51] Serrano, S. E. 1990. Modeling infiltration in hysteretic soils. *Advances in Water Resources,* 13(1): 12-23. DOI: https://doi.org/10.1016/0309-1708(90)90034-2.

[52] Šimůnek, J., van Genuchten, M. Th., & Šejna, M. 2012. The Hydrus software package for simulating two- and three-dimensional movement of water, heat, and multiple solutes in variably-saturated media, version 2.0. Prague, Czech Republic: PC Progress.

[53] Song, X., & Borja, R. I. 2014. Mathematical framework for unsaturated flow in the finite deformation range. *International Journal for Numerical Methods in Engineerin*g, 97(9): 658-682. DOI: https://doi.org/10.1002/nme.4603.

[54] Stonestrom, D. A., & Rubin, J. 1989. Water-content dependence of trapped air in two soils. *Water Resources Research*, 25(9): 1947-1958. DOI: https://doi.org/10.1029/WR025i009p01947.

[55] Sun, D., Sheng, D., & Sloan, S. W. 2007. Elastoplastic modelling of hydraulic and stress-strain behaviour of unsaturated soils. *Mechanics of Materials,* 39(3): 212-221. DOI: https://doi.org/10.1016/j.mechmat.2006.05.002.

[56] Sun, D. M., Zang, Y. G., Feng, P. F., & Semprich, S. 2016. Quasi-saturated zones induced by rainfall infiltration. *Transport in Porous Media,* 112(1): 77-104. DOI: https://doi.org/10.1007/s11242-016-0633-y.

[57] Tami, D., Rahardjo, H., & Leong, E.-C. 2004. Effects of hysteresis on steady-state infiltration in unsaturated slopes. *Journal of Geotechnical and Geoenvironmental Engineering*, 130(9): 956-967. DOI: https://doi.org/10.1061/(ASCE)1090-0241(2004)130:9(956).

[58] Toyota, H., Nakamura, K., Sakai, N., & Sramoon, W. 2003. Mechanical Properties of Unsaturated Cohesive Soil in Consideration of Tensile Stress. *Soils and Foundations,* 43(2): 115-122. DOI: https://doi.org/10.1016/S0038-0806(20)30806-4.

[59] Vachaud, G., & Thony, J.-L. 1971. Hysteresis during infiltration and redistribution in a soil column at different initial water contents. *Water Resources Research,* 7(1): 111-127. DOI: https://doi.org/10.1029/WR007i001p00111.

[60] van Genuchten, M. Th. 1980. A closed-form equation for predicting the hydraulic conductivity of unsaturated soils. *Soil Science Society of America Journal,* 44(5): 892-898. DOI: https://doi.org/10.2136/sssaj1980.03615995004400050002x.

[61] Wei, C., & Dewoolkar, M. M. 2006. Formulation of capillary hysteresis with internal state variables. *Water Resources Research*, 42(7): W07405. DOI: https://doi.org/10.1029/2005WR004594.

[62] Werner, A. D., & Lockington, D. A. 2006. Artificial pumping errors in the Kool-Parker scaling model of soil moisture hysteresis. Journal of Hydrology, 325(1-4): 118-133. DOI: https://doi.org/10.1016/j.jhydrol.2005.10.012.

[63] Wheeler, S. J., Sharma, R. S., & Buisson, M. S. R. 2003. Coupling of hydraulic hysteresis and stress-strain behaviour in unsaturated soils. *Géotechnique,* 53(1): 41-54. DOI: https://doi.org/10.1680/geot.2003.53.1.41.

[64] Yang, C., Sheng, D., & Carter, J. P. 2012. Effect of hydraulic hysteresis on seepage analysis for unsaturated soils. *Computers and Geotechnics,* 41: 36-56. DOI: https://doi.org/10.1016/j.compgeo.2011.11.006.

[65] Zhou, A. 2017. Modelling hydro-mechanical behavior for unsaturated soils. *Japanese Geotechnical Society Special Publication*, 5(2): 79-94. DOI: https://doi.org/10.3208/jgssp.v05.019.

.